

### 3.11 Comparison of the DM Treatment with Vector Representation

It is now possible to follow the 2DHETCOR vector representation (Figures I.6a through I.6d) and identify each step with the corresponding density matrix. It will be seen that one cannot draw the vectors for the entire sequence without the knowledge of the DM results.

As demonstrated in Appendix B (see B15-B22) the magnetization components at any time are given by:

$$M_{zA} = -(2M_{oA} / p)(d_{11} - d_{22} + d_{33} - d_{44}) \quad (\text{B15})$$

$$M_{zX} = -(2M_{oX} / q)(d_{11} - d_{33} + d_{22} - d_{44}) \quad (\text{B21})$$

$$M_{TA} = -(4M_{oA} / p)(d_{12}^* + d_{34}^*) \quad (\text{B20})$$

$$M_{TX} = -(4M_{oX} / q)(d_{13}^* + d_{24}^*) \quad (\text{B22})$$

Considering the simplification we made in (I.7), we must multiply the expressions above with the factor  $p/4$ . Also, remembering that for the CH system  $q = 4p$ , we obtain

$$\begin{aligned} M_{zC} &= -(M_{oC} / 2)(d_{11} - d_{22} + d_{33} - d_{44}) \\ M_{zH} &= -(M_{oH} / 8)(d_{11} - d_{33} + d_{22} - d_{44}) \\ M_{TC} &= -M_{oC}(d_{12}^* + d_{34}^*) \\ M_{TH} &= -(M_{oH} / 4)(d_{13}^* + d_{24}^*) \end{aligned} \quad (\text{I.53})$$

We will use the relations (I.53) throughout the sequence in order to find the magnetization components from the matrix elements.

At time  $t(0)$  the net magnetization is in the  $z$ -direction for both proton and carbon. Indeed, with the matrix elements of  $D(0)$  (see I.7) we find

$$\begin{aligned} M_{zC} &= -(M_{oC} / 2)(0 - 1 + 4 - 5) = +M_{oC} \\ M_{zH} &= -(M_{oH} / 8)(0 - 4 + 1 - 5) = +M_{oH} \end{aligned} \quad (\text{I.54})$$

The transverse magnetizations  $M_{TC}$  and  $M_{TH}$  are both zero (all off-diagonal elements are zero), consistent with the fact that no pulse has been applied.

Although they are indiscernible at thermal equilibrium, we will now define *fast* and *slow* components using Figure I.5.

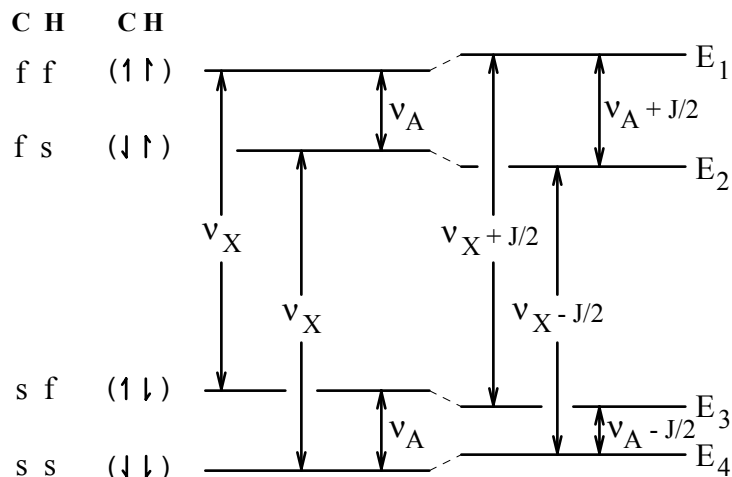


**Figure I.5.** *Fast* and *slow* labeling.

It is seen that protons in states 1 and 3 cannot be involved but in the higher frequency transition 1 – 3, i.e., they are *fast*. Those in states 2 and 4 are *slow*. Likewise, carbons in states 1 and 2 are *fast*, those in states 3 and 4 are *slow*. Therefore, according to (I.53) and (I.54), at  $t(0)$  half of  $M_{zH}$  is due to *fast* protons ( $d_{11} - d_{33}$ ) and the other half to *slow* protons. The *fast* and *slow* components of the proton magnetization are marked in Figure I.6 with 13 and 24, respectively. For carbon, it is 12 and 34.

Speaking of C-H pairs, a proton can add or subtract to the field "seen" by the carbon. Therefore the carbon will be *fast* if it pairs with a spin-up proton or *slow* if it pairs with a spin-down proton. The carbon spins will have a similar effect on protons. Figure I.5 shows that the spins become *faster* or *slower* by  $J/2$  Hz.

Immediately after the  $90xH$  pulse proton coherences were created. Using the matrix elements of  $D(1)$  (see I.12) we obtain:

$$M_{TH} = -(M_{oH} / 4)(2i + 2i) = -iM_{oH}$$

This tells us that the pulse brought the proton magnetization on the  $-y$ -axis (the reader is reminded that in the transverse magnetization,  $M_T = M_x + iM_y$ , the real part represents vectors along the  $x$ -axis and the imaginary part vectors along the  $y$ -axis). It can be verified that the longitudinal proton magnetization is zero since  $d_{11} - d_{22} + d_{33} - d_{44} = 2 - 2 + 3 - 3 = 0$  (cf I.53). The carbon magnetization was not affected [Figure I.6a  $t(1)$ ].

The chemical shift evolution  $\Omega_H t_e / 2$  is the average of the fast and slow evolutions discussed above [see (I.23 – 24)]. The vector 13 is ahead by  $+\pi J t_e / 2$ , while 24 is lagging by the same angle (i.e.,  $-\pi J t_e / 2$ ). The DM results [see (I.14 – 16)] demonstrate the same thing:

$$\begin{aligned} M_{TH} &= -(M_{oH} / 4)(B^* + C^*) \\ &= -(M_{oH} / 4)[2i \exp(i\Omega_{13} t_e / 2) + 2i \exp(i\Omega_{24} t_e / 2)] \\ &= -i(M_{oH} / 4) \exp(i\Omega_H t_e / 2) [\exp(i\pi J t_e / 2) + \exp(-i\pi J t_e / 2)] \end{aligned}$$

The carbon is still not affected [Figure I.6a  $t(2)$ ].

Figure I.6b  $t(3)$  tells us that the  $180^\circ C$  pulse reverses the carbon magnetization and also reverses the proton labels. As discussed above, the protons coupled to *up* carbons are fast and those coupled to *down* carbons are slow. Therefore inverting carbon orientation results in changing fast protons into slow protons and vice versa. This is mathematically documented in the DM treatment [see (I.20)]. The matrix element  $B$  is transferred in the slow (24) "slot" and will evolve from now on with the *slow* frequency  $\Omega_{24}$ . The reverse is happening to the matrix element  $C$ . The longitudinal carbon magnetization changed sign:

$$-(d_{11} - d_{22} + d_{33} - d_{44}) = -(3 - 2 + 3 - 2) = -2$$

Figure I.6b  $t(4)$  clearly shows that the second evolution  $t_e / 2$  completes the decoupling of proton from carbon. The fast vector 13 catches up with the slow 24 and at  $t(4)$  they coincide. They have both precessed a total angle  $\Omega_H t_e$  from their starting position along  $-y$ . We can verify that the matrix elements  $d_{13}^*$  and  $d_{24}^*$  are equal at  $t(4)$  [see (I.25) and (I.26)]. The transverse magnetization, calculated from the matrix elements, is

$$M_{TH} = -(M_{oH} / 4)[2i \exp(i\Omega_H t_e) + 2i \exp(i\Omega_H t_e)] = -iM_{oH} \exp(i\Omega_H t_e)$$

After separating the real and imaginary parts in  $M_{TH}$  we obtain

$$\begin{aligned} M_{TH} &= -iM_{oH}(\cos \Omega_H t_e + i \sin \Omega_H t_e) = M_{oH}(\sin \Omega_H t_e - i \cos \Omega_H t_e) \\ M_{xH} &= \text{real part of } M_{TH} = M_{oH} \sin \Omega_H t_e \\ M_{yH} &= \text{coefficient of the imaginary part of } M_{TH} = -M_{oH} \cos \Omega_H t_e \end{aligned}$$

This is in full accordance with the vector representation. The carbon magnetization is still along  $-z$ .

Figure I.6b  $t(5)$  shows what happened during the delay  $\Delta_1$  which has been chosen equal to  $1/2J$ . Each of the two proton magnetization components rotated by an angle  $\Omega_H \Delta_1$  but, with respect to the average, the fast component has gained  $\pi/2$  while the slow one has lost  $\pi/2$ . As a result, the vectors are now opposite. We can verify [see (I.30)] that at  $t(5)$  the elements  $d_{13}$  and  $d_{24}$  are equal and of opposite signs. The carbon magnetization did not change.

Figure I.6c shows the situation at  $t(6)$ , after the  $90xH$  pulse. When we went through the DM treatment, we combined the last two pulses into a single rotation operator and this brought us directly from  $D(5)$  to  $D(7)$ . However, for the comparison with the vector representation and for an understanding of the polarization transfer, it is necessary to discuss the density matrix  $D(6)$ . It can be calculated by applying the rotation operator  $R_{90xH}$  [see (I.9)] to  $D(5)$  given in (I.33). The result is

$$D(6) = \begin{bmatrix} 3-2s & 0 & -2c & 0 \\ 0 & 2+2s & 0 & 2c \\ -2c & 0 & 3+2s & 0 \\ 0 & 2c & 0 & 2-2s \end{bmatrix} \quad (\text{I.55})$$

The magnetization components in Figure I.6c are derived from the matrix elements of  $D(6)$ , using (I.53). What happens to the proton magnetization can be predicted from the previous vector representation but *what happens to the carbon cannot*. As far as the proton is concerned, its  $x$  components are not affected, while the other components rotate from  $y$  to  $z$  and from  $-y$  to  $-z$ , as expected after a  $90x$  pulse.

The net longitudinal carbon magnetization does not change, it is still  $-M_{oC}$ , but a sizable imbalance is created between its fast and slow components:

$$\begin{aligned} M_{12} &= -(M_{oC}/2)(d_{11} - d_{22}) = -(M_{oC}/2)(3 - 2s - 2 - 2s) \\ &= M_{oC}(-1/2 + 2s) \end{aligned} \quad (I.56)$$

$$\begin{aligned} M_{34} &= -(M_{oC}/2)(d_{33} - d_{44}) = -(M_{oC}/2)(3 + 2s - 2 + 2s) \\ &= M_{oC}(-1/2 - 2s) \end{aligned} \quad (I.57)$$

$$M_{zC} = M_{12} + M_{34} = -M_{oC} \quad (I.58)$$

The imbalance term is proportional to  $s = \sin[\Omega_H(t_e + \Delta_1)]$ , i.e, it is proton modulated. When  $s$  varies from +1 to  $-1$ , the quantity  $2sM_{oC}$  varies from  $+2M_{oC}$  to  $-2M_{oC}$ , a swing of  $4M_{oC}$ . The remaining of the sequence is designed to make this modulated term observable.

For  $s$  greater than 1/4,  $M_{12}$  becomes positive while  $M_{34}$  remains negative. In other words, the fast carbons are now predominantly up and the slow ones predominantly down. A correlation has been created between the *up-down* and the *fast-slow* quality of the carbon spins. The Figure I.6c is drawn for  $s \cong 0.95$

The last pulse of the sequence, a  $90x_C$ , brings us to  $D(7)$  [see (I.35)] and to Figure I.6d  $t(7)$ . It is seen that the vector representation can explain how carbon magnetization is affected by the pulse (12 goes in  $-y$  and 34 in  $+y$ ), but *it cannot explain the nulling of proton magnetization*. Note that from  $t(5)$  on, the net magnetization was zero (opposite vectors) but now 13 and 24 are null themselves. The density matrix  $D(7)$  [see(I.35)] shows

$$\begin{aligned} M_{T12} &= iM_{oC}(1/2 - 2s) \\ M_{T34} &= iM_{oC}(1/2 + 2s) \end{aligned}$$

Separation of the real and imaginary parts gives

$$\begin{aligned} M_{x12} &= 0 & ; & & M_{y12} &= M_{oC}(1/2 - 2s) \\ M_{x34} &= 0 & ; & & M_{y34} &= M_{oC}(1/2 + 2s) \end{aligned}$$

The net carbon magnetization is

$$M_{xC} = M_{x12} + M_{x34} = 0$$

$$M_{yC} = M_{y12} + M_{y34} = M_{oC}$$

The proton modulated term,  $2s$ , is not yet observable (it does not appear in  $M_{xC}$  or  $M_{yC}$ ). The delay  $\Delta_2$  will render it observable. We see in Figure I.6d  $t(8)$  that the two components have rotated by an average of  $\Omega_C \Delta_2$ . The fast one has gained  $\pi/2$  and the slow one has lost  $\pi/2$ . As a result, the two vectors (of unequal magnitude) are now coincident. Relations (I.42) and (I.43) confirm that at time  $t(8)$  both matrix elements  $d_{12}^*$  and  $d_{34}^*$  have the same phase factor,  $\exp(i\Omega_C \Delta_2)$ . The net carbon magnetization is

$$\begin{aligned} M_{TC} &= -M_{oTC} (d_{12}^* + d_{34}^*) = -M_{oC} (1/2 - 2s - 1/2 - 2s) \exp(i\Omega_C \Delta_2) \\ &= 4sM_{oC} \exp(i\Omega_C \Delta_2) \end{aligned} \quad (I.59)$$

The factor 4 in (I.59) represents the enhancement of the carbon magnetization by polarization transfer. This could not be even guessed from the vector representation.

Nothing remarkable happens after the end of  $\Delta_2$ . The proton decoupler is turned on and the carbon magnetization is precessing as a whole during the detection time  $t_d$  (no spreadout of the fast and slow components).

This is the end of the vector representation of the 2DHETCOR sequence. Such representation would not have been possible without the *complete* information provided by the DM treatment.

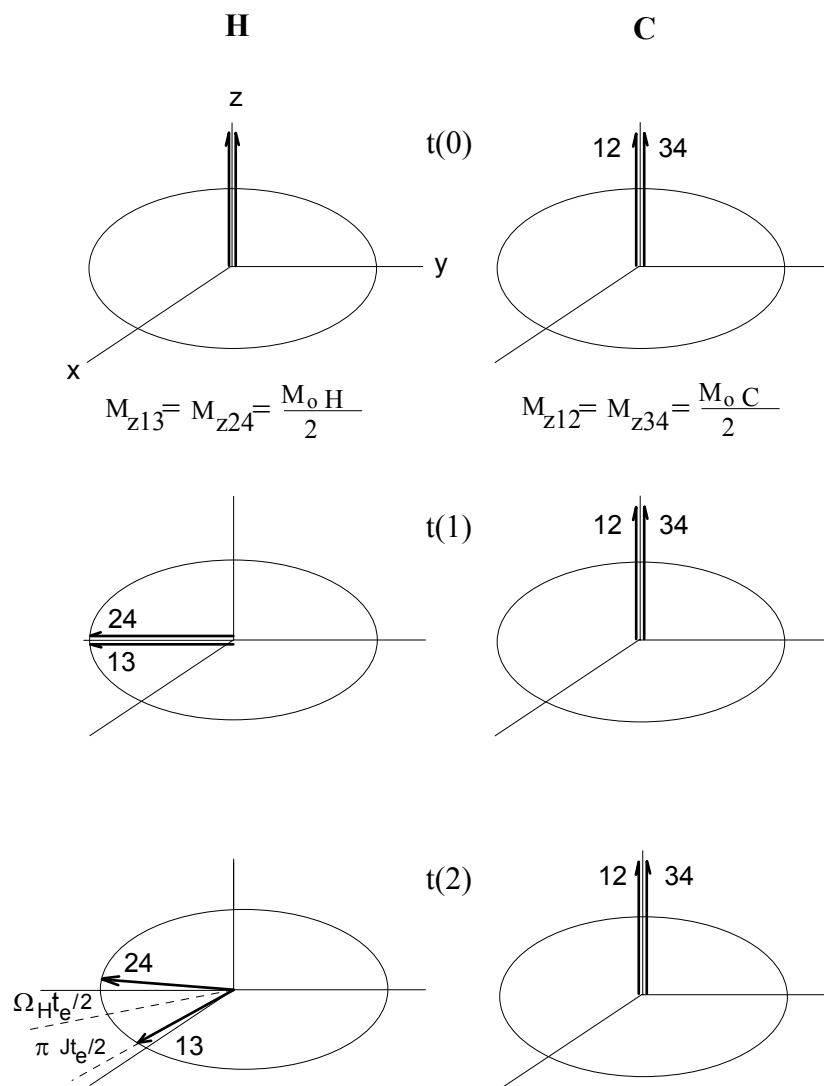


**Figure I.6a.** Vector representation of 2DHETCOR from  $t(0)$  to  $t(2)$ . The magnetization vectors are arbitrarily taken equal for C and H in order to simplify the drawing. Actually the  $^1\text{H}$  magnetization at equilibrium is 16 times larger than that of  $^{13}\text{C}$ .

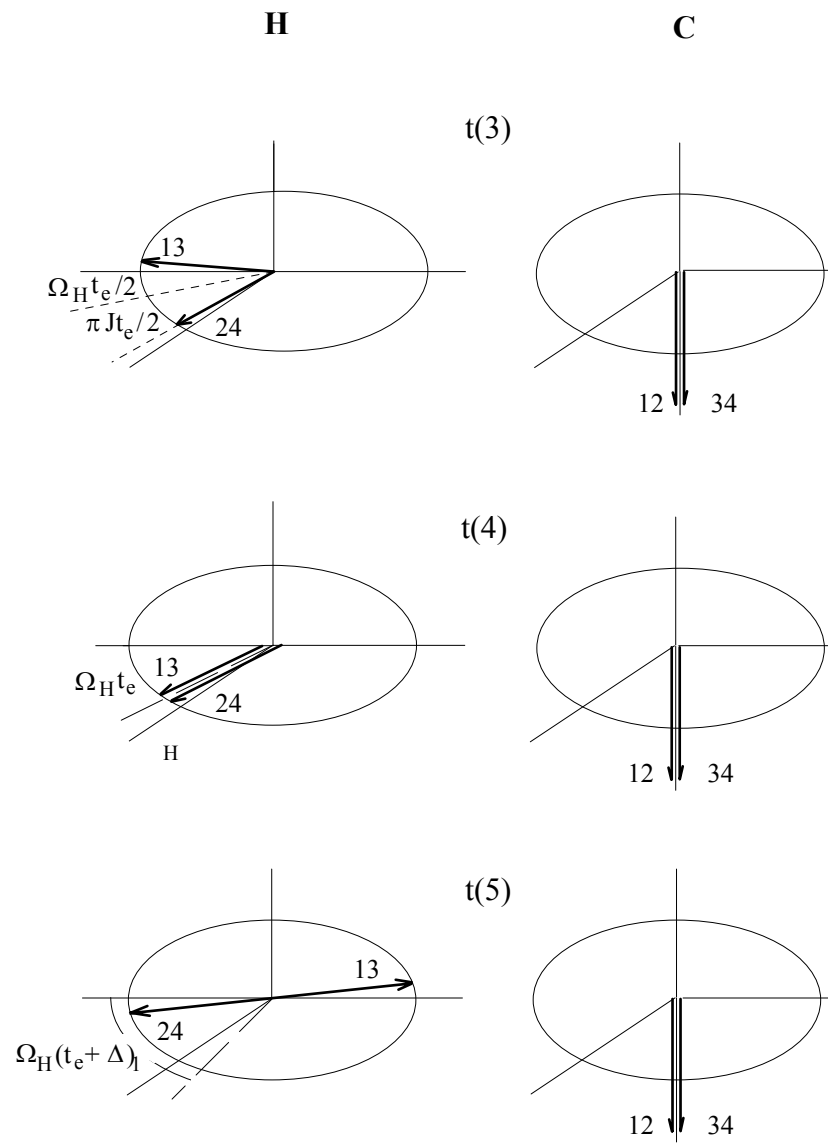


**Figure I.6b.** Vector representation of 2DHETCOR from  $t(3)$  to  $t(5)$ .

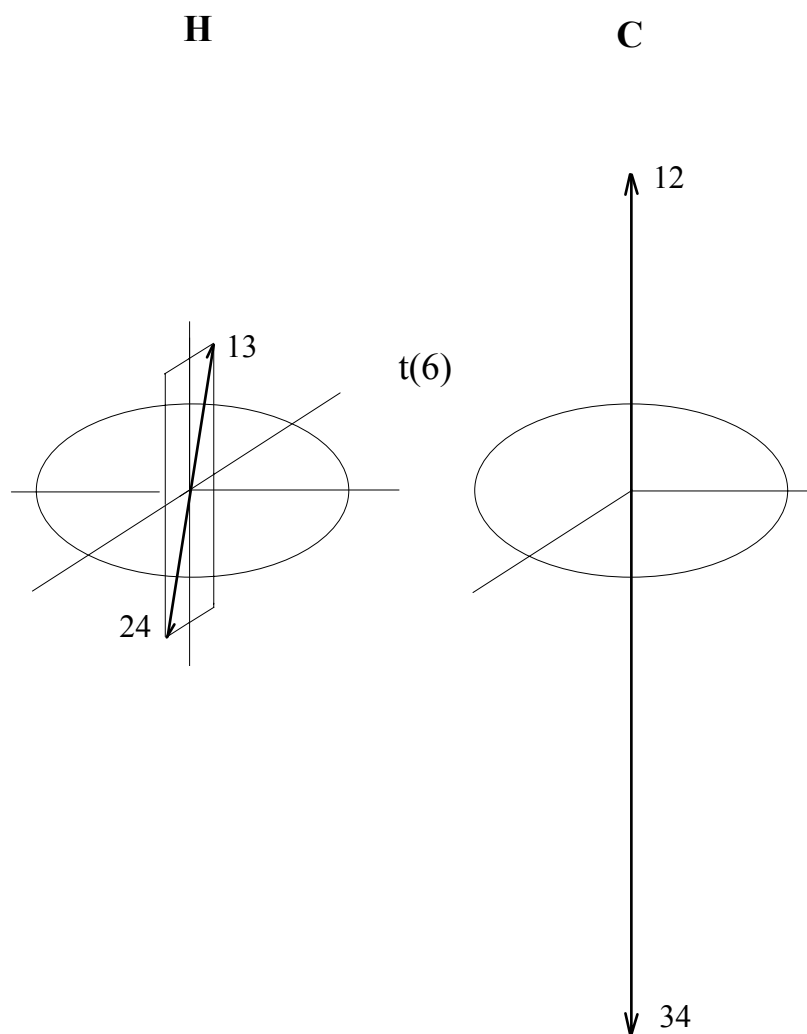


**Figure I.6c.** Vector representation of 2DHETCOR at time  $t(6)$ . The carbon magnetization components depend on the value of  $s$  (they are proton modulated):

$$M_{z12} = -(1 - 4s)M_{oC} / 2$$

$$M_{z34} = -(1 + 4s)M_{oC} / 2$$

$$s = \sin \Omega_H (t_e + \Delta_1)$$

The figure is drawn for  $s \cong 0.95$ .

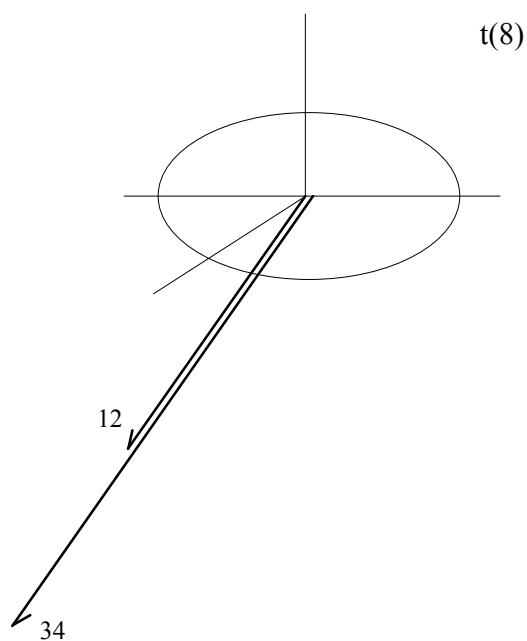
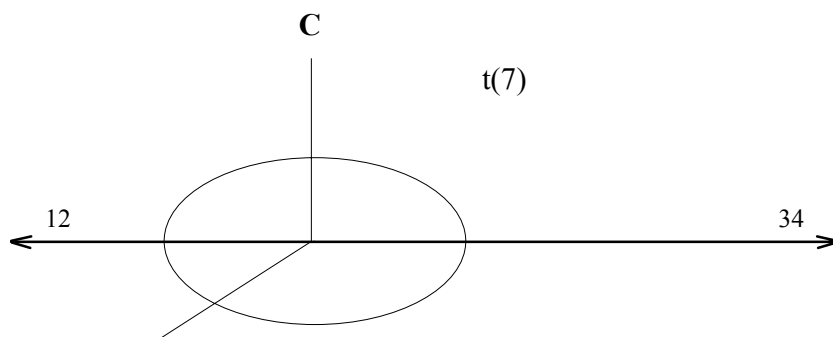


**Figure 1.6d.** Vector representation of 2DHETCOR at  $t(7)$  and  $t(8)$ .

The carbon magnetization components at  $t(7)$  are

$$M_{y12} = (1 - 4s) M_{oC} / 2$$

$$M_{y34} = (1 + 4s) M_{oC} / 2 \quad s = \sin \Omega_H (t_e + \Delta_1)$$

The proton magnetization components, both fast and slow, have vanished.